Sensitivity Analyses of Satellite Rainfall Retrieval and Sampling Error on Flood Prediction Uncertainty

Faisal Hossain, Emmanouil N. Anagnostou, and Tufa Dinku

***Abstract*—The Global Precipitation Measurement mission planned jointly by the United States, Japanese, and European space agencies envisions providing global rainfall products from a constellation of passive microwave (PM) satellite sensors at time scales ranging from 3–6 h. In this paper, a sensitivity analysis was carried out to understand the implication of satellite PM rainfall retrieval and sampling errors on flood prediction uncertainty for medium-sized ($\sim$ 100 km^2) watersheds. The 3-h rainfall sampling gave comparable flood prediction uncertainties with respect to the hourly sampling, typically used in runoff modeling, for a major flood event in Northern Italy. The runoff prediction error, though, was magnified up to a factor of 3 when rainfall estimates were derived from 6-h PM sampling intervals. The systematic and random error components in PM retrieval are shown to interact with PM sampling introducing added uncertainty in runoff simulation. The temporal correlation in the PM retrieval error was found to have a negligible effect in runoff prediction. It is shown that merging rain retrievals from hourly infrared (IR) and PM observations generally reduces flood prediction uncertainty. The error reduction varied between 50% (0%) and 80% (50%) for the 6-h (3-h) PM sampling scenarios, depending on the relative magnitudes of PM and IR retrieval errors. Findings from this paper are potentially useful for the design, planning, and application assessment of satellite remote sensing in flood and flash flood forecasting.**

***Index Terms*—Flood prediction uncertainty, infrared, passive microwave, rainfall retrieval error.**

I. Introduction

PASSIVE microwave (PM) radiometers for remote sensing of rainfall have shown great promise because of the direct interaction between hydrometeors and the radiation field. Unlike infrared (IR) measurements, which are sensitive only to the uppermost layer of clouds, PM radiation has the ability to penetrate the clouds offering insight into the structure of rainfall itself. PM sensors have flown on a number of spaceborne platforms. In 1987, the first Special Sensor Microwave/Imager (SSM/I) was launched on the Defense Meteorological Satellite Program (DMSP) F-8 satellite. Currently, there are three SSM/I spacecrafts (F13, F14, and F15) providing PM rainfall retrievals in sun-synchronous orbits. In 1997, the Tropical Rainfall Measuring Mission (TRMM) was launched. TRMM carries a Microwave Imager (TMI) similar to the SSM/I [1]. Very recently, another PM sensor for rainfall retrieval, the Advanced Microwave Scanning Radiometer for EOS (AMSR-E) was launched in 2002 as part of the AQUA mission [2].

The particular success of TRMM in improving our understanding on tropical and subtropical rainfall distribution and precipitation structures has now spurred a larger scale mission aimed at the study of global water cycle. This mission, named the Global Precipitation Measurement (GPM), envisions a constellation of PM sensors that will provide global rainfall products at scales ranging from 3–6 h over regions as small as 100 km^2 [3]–[6]. GPM also envisions the extension of "scientific and societal applications" of this high-resolution global rainfall data as one of its major objectives [5]. Previous uses of PM rainfall retrievals include weather forecasting, climate analysis, and large-scale hydrologic studies [7]–[11].

The enhanced revisit frequency and global coverage of PM sensors as planned in GPM will make for the first time PM retrievals attractive for the prediction of floods over ungauged watersheds. This is extremely important, as flood is the deadliest and economically most destructive natural hazard; more than 2000 lives are lost and at least 10 000 000 people are displaced annually since 1991 (see www.dartmouth.edu/~floods). Most importantly, floods are more frequent in regions that lack financial resources to employ networks of surface weather stations necessary for flood monitoring. Thus, observations from satellite sensors stand to offer tremendous benefit to such ungauged areas.

However, PM rainfall retrieval is subject to errors caused by various factors ranging from instrument issues (e.g., calibration, measurement noise) to the high complexity and variability in the relationship of brightness temperatures to precipitation parameters. It is documented that any presence of error in remote sensing of rainfall can potentially lead to high uncertainties in the simulation of runoff at the watershed scale [12]–[14]. Guetter *et al.* [15] have found that satellite retrieval errors propagated through a hydrologic model forced with satellite data can yield significant uncertainty in the prediction of hydrologic parameters. Hossain *et al.* [14] show that the systematic and random components of a rain retrieval algorithm would interact nonlinearly with the hydrologic modeling uncertainty, leading to a high uncertainty in the resulting flood forecasts. Hence, we need to understand the sensitivity of flood prediction uncertainty to the error characteristics of the satellite rainfall retrievals that are used as input to the hydrological model.

Furthermore, as space-based sampling from PM sensors is less frequent than the hourly scale typically used in most types of flood prediction [3], it would be important to study the effect of infrequent sampling (hereafter named sampling error)

Manuscript received April, 22, 2003; revised August 15, 2003. This work was supported by the National Aeronautics and Space Administration (NASA) under New Investigator Award NAG5-8636. The work of F. Hossain was supported by the NASA Earth System Science Graduate Fellowship under Award NASA ESSF/02-0000-0047.

The authors are with the Department of Civil and Environmental Engineering, University of Connecticut, Storrs, CT 06269 USA (e-mail: faisal@engr.uconn.edu; manos@engr.uconn.edu; tufad@engr.uconn.edu).

Digital Object Identifier 10.1109/TGRS.2003.818341

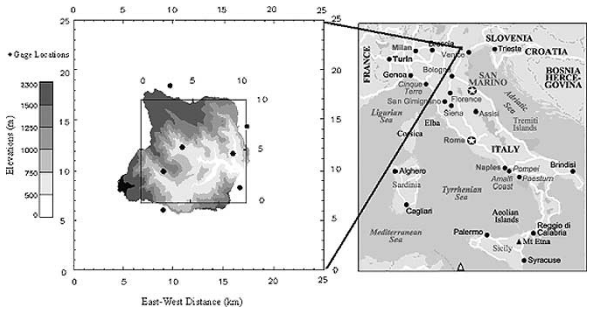

Fig. 1. Geographic location of (right panel) Posina watershed and (left panel) watershed elevation map overlaid by the rain gauge network locations (in solid circles). The inner box represents a typical 10 × 10 km satellite footprint.

ranging from 6 h (average current conditions) to 3 h (average planned for GPM constellation) on flood prediction uncertainty. In contrast to PM sensors, IR radiometers on geosynchronous satellites provide excellent time and space sampling, but the remotely sensed parameter (primarily cloud-top brightness temperature) is connected loosely to the physics of rainfall below. Hence, it is also worthwhile investigating the utility of the less definitive IR rainfall retrievals in conjunction with PM retrievals for flood prediction. The specific questions that this paper seeks to address are: 1) *How do factors of PM sampling (3- and 6-h) and retrieval error characteristics interact in the runoff transformation process at the watershed scale and contribute to flood prediction uncertainty?* 2) *What is the impact of using combined IR and PM retrievals at hourly time scales on flood prediction uncertainty?* With the anticipated wider availability of satellite rainfall products from GPM, this paper is probably the first of the many required to answer the bigger question facing the hydrologic community today: *What combination and levels of uncertainty of multisensor satellite rainfall retrievals are necessary to achieve realistic flood predictions?*

Section II provides a description of the data, the watershed and hydrologic model used for flood prediction. Section III describes the formulation of a satellite rainfall retrieval error model. This error model is necessary in making multiple simulated realizations of the rainfall process as would have been typically observed by a constellation of satellite sensors (PM and IR) during a storm event. In Section IV, the simulation framework used to investigate the sensitivity of sampling and retrieval error characteristics in flood prediction uncertainty are described. Results and discussion of the implications of this paper are also provided in this section. Section V describes our conclusions and discusses extensions of this paper.

II. Watershed, Data, and Hydrologic Model

The watershed chosen for this paper (named Posina) is located in northern Italy, close to Venice (Fig. 1, right panel). Posina has an area of 116 km^2 and altitudes ranging from 2230–390 m at the outlet (Fig. 1, left panel). Within a radius of 10 km from the center of the watershed there is a network of seven rain gauges providing representative estimates of the basin-averaged hourly rainfall (hereafter referred to as "*reference rainfall*"). This is considered a relatively dense network considering that a previous hydrologic application study of satellite data by [15] involved much less dense network of 29

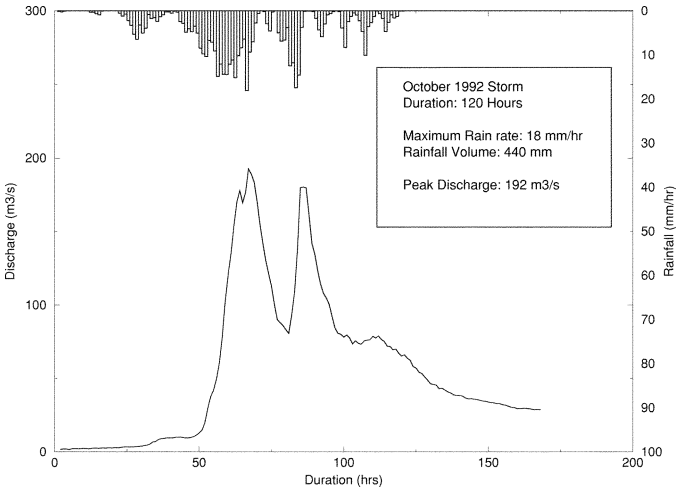

Fig. 2. October 1992 storm event hydrograph and hyetograph in Posina, Italy.

gauges over watersheds larger than 2000 km^2. The estimation of basin-averaged rainfall was based on an inverse distance weighting technique that had earlier proved to be a reliable method for similar hydrologic studies over Posina [13], [14], [16]. The annual precipitation accumulation is estimated to be in the range of 1600–1800 mm. Posina is 68% forested, thereby saturation-excess is the main rainfall-runoff generation mechanism of the basin. A major storm event that took place in October 1992 and was associated with catastrophic flooding in the area was selected for this paper [13]. Fig. 2 shows the storm hydrograph (lower axis) and the corresponding hourly basin-averaged gauge rainfall (upper axis). The rainfall event lasted 120 h (five days), while the flood wave receded to the base flow level on the seventh day (after 168 h from the beginning of the storm). The meteorological situation associated with such a storm system was characterized by cyclogenesis in the surrounding region, which often occurs over western Mediterranean in autumn months [17]. Further details about the study area, including its terrain characteristics and rain climatology can be found in [13].

The topographic index model (TOPMODEL) [18] was chosen to simulate the rainfall-runoff processes of the Posina watershed. This model is a semi distributed watershed model that can simulate the variable source area mechanism of storm-runoff generation and incorporates the effect of topography on flow paths. TOPMODEL makes a number of simplifying assumptions about the runoff generation processes that are thought to be reasonably valid in this wet, humid watershed. The model is premised on the following two assumptions: 1) the dynamics of the saturated zone can be approximated by successive steady state representations; and 2) the hydraulic gradient of the saturated zone can be approximated by the local surface topographic slope. The generated runoff is routed to the main channel using an overland flow delay function. The main channel routing effects are considered using an approach based on an average flood wave velocity for the channel network. Detailed background information of the model and applications can be found in [19]. The model has been successfully applied in the study region by previous hydrologic studies in [13] and [14].

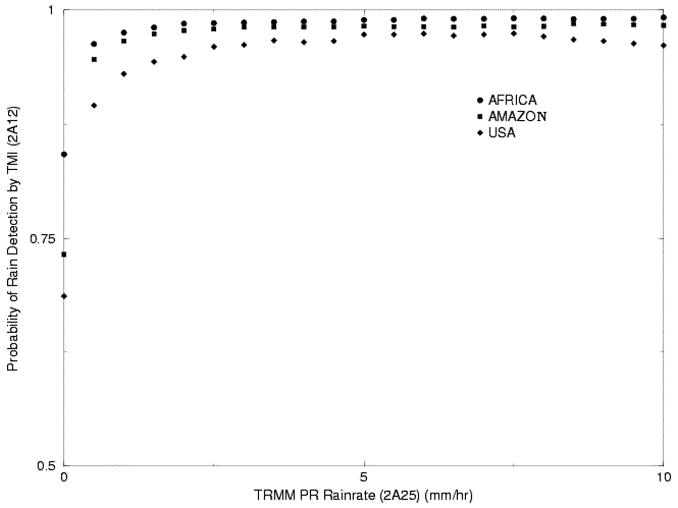

Fig. 3. Probability of rain detection by PM (TMI) retrievals over Southern Africa, Amazon and the Southern United States determined using TRMM Precipitation Radar (PR) surface rainfall estimates as reference. The data products used for TRMM PR and TMI rain rates were 2A25 and 2A12, respectively. The period of matched PR/TMI data was January–July 2002.

III. Satellite Rainfall Error Model

We formulated a *satellite rainfall error model* (SREM) to simulate PM and IR satellite rainfall retrievals by corrupting more accurate sources of "*reference*" surface rainfall, in this study provided by a dense rain gauge network. The utility of this model was then in its ability to mimic basin-averaged rainfall retrievals from hypothetical satellite observations over the Posina basin. Rain retrieval from a satellite observation may exhibit the following possible outcomes.

1) It retrieves nonzero rainfall when *reference rainfall* is nonzero (successful rain detection).
2) It retrieves zero rainfall when *reference rainfall* is nonzero (false no-rain detection).
3) It retrieves zero rainfall when *reference rainfall* is zero (successful no-rain detection).
4) It retrieves nonzero rainfall when *reference rainfall* is zero (false rain detection).

We define the successful rain detection probability (first outcome), $P_1 = \text{Prob}(R_{\text{SAT}} > 0 | R_{\text{REF}} > 0)$, as function of the reference rainfall

$$P_1 = 1.0 - \lambda_O \exp(-\lambda R_{\text{REF}}) \tag{1}$$

where λ_0 and λ are parameters to be derived from boundary condition values of the rain detection probability. The false no-rain detection probability (second outcome) is consequently defined as $1 - P_1$. The choice for an exponential-type function for P_1 was on the basis of real data as shown in Fig. 3, derived from TRMM radar/TMI radiometer rain product comparisons over different sites on the globe. Fig. 3 shows that the rain detection probability of TMI retrieval converges to near 1 when the *reference* rain rate (in this case, reference rainfall is inferred for TRMM precipitation radar [1]) exceeds 5 mm/h. However, for the IR rain retrieval this threshold rain rate can take a wide range of values depending on the retrieval algorithm and resolution (in this paper, we assume the value being twice the PM threshold value, i.e., 10 mm/h). A very low probability of detection (0.001) is given to the PM rain detection probability, $P_{1\text{PM}}$, when *reference* rainfall is below 0.2 mm/h, while the corresponding value for IR rain algorithms was set to 0.8 mm/h. The values of $\lambda_0(\lambda)$ satisfying the above boundary conditions were therefore found to be 1.332 (1.439) and 1.821 (0.751) for PM and IR retrievals, respectively. In low rain rates (below 1 mm/h), there is a slight discrepancy between detection probabilities derived from data versus the model of (1). Since the storm of this paper is associated with rain rates significantly higher of the above threshold (see Fig. 2, upper axis) we expect this discrepancy to have little effect on the flood prediction uncertainty assessment. The justification for assigning a significantly less accurate IR rain detection capability is based on a number of reasons. First, IR retrievals tend to suffer from a spatial and temporal offset that often lowers its rain detection probability at scales relevant to this study [20]. Typically, IR retrievals are not always suited to detection of very light rain [21]. An algorithm intercomparison study by Negri and Adler [24] found that IR rain retrievals have poor performance at hourly time scales. Another study by [22] reported that IR retrievals can have a rain detection probability of 0.64 for rain rates ranging between 0–2 mm/h, which is quantitatively consistent with the detection probability derived from (1) using upper and lower IR rain detection thresholds of 0.2 and 10 mm/h, respectively.

We define the successful no-rain detection probability (third outcome) of the satellite retrieval as $P_0 = \text{Prob}(R_{\text{SAT}} = 0 | R_{\text{REF}} = 0)$, while $1 - P_0$ defines the false rain detection probability (fourth outcome). The probability P_0 was defined to be high for PM retrievals (0.98) as shown in [7], while for IR it was given a lower value (0.90). The lower value of no rain detection for IR was based on results from a previous hydrologic study [23] that reported a value of 0.92 on the basis of comparisons with area-averaged gauge rainfall over a midlatitude basin in the United States.

Our next step is to assign rainfall rate values in the first and fourth outcome where the satellite retrieval is nonzero. In the first outcome, the retrieved satellite rain rate R_{SAT} is statistically related to the *reference* surface rainfall R_{REF} as

$$R_{\text{SAT}} = R_{\text{REF}} \cdot \varepsilon_{\text{S}} \tag{2}$$

where the multiplicative satellite error parameter ε_{s} is assumed log-normally distributed. A log transformation of the $\log(R_{\text{SAT}}) - \log(R_{\text{REF}})$ statistical relationship transforms the error ε_s to a Gaussian deviate ε (hereafter named "log-error") with $N(\mu, \sigma^2)$ statistics (μ – mean; σ^2 – variance). To compute the mean (hereafter named "multiplicative bias" – mu) and variance (S^2) of the multiplicative error ε_s the following conversion is used in terms of μ and σ^2

$$mu = \exp(\mu + 0.5\sigma^2) \tag{3}$$

$$S^2 = [\exp(\sigma^2) - 1] \exp(2\mu + \sigma^2). \tag{4}$$

The log-error can be space and time correlated. Only time correlation was considered due to the nature of this study, i.e., the basin-averaged rainfall is represented by a single PM rain retrieval pixel, which is expected to be of the order of about 10×10 km^2 resolution for GPM [6]. A lag-one autocorrelation function was used to model the correlated error sequence, which

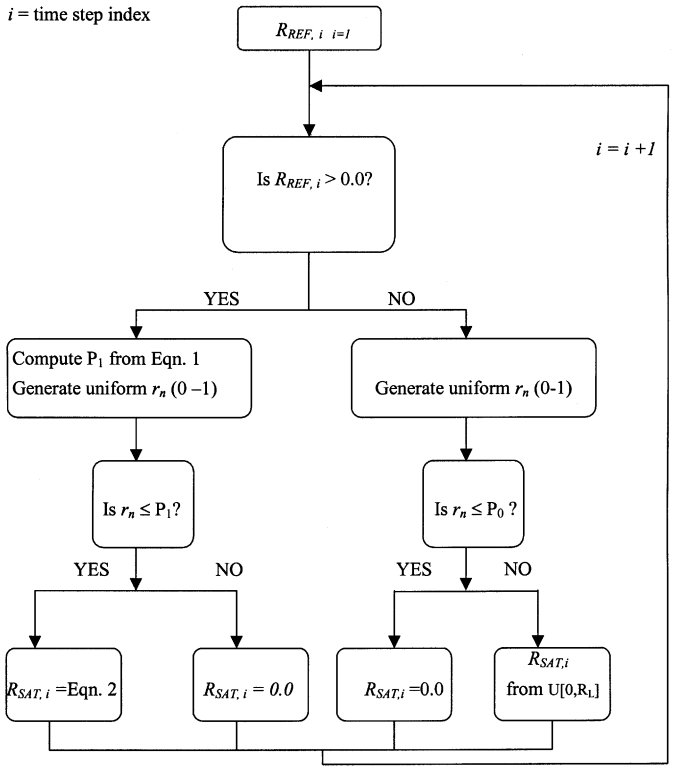

Fig. 4. Algorithmic structure of the SREM. r_n is a randomly generated uniform [0,1] deviate.

TABLE I

(a) RAIN DETECTION AND NO-RAIN DETECTION PROBABILITIES FOR IR AND PM RETRIEVALS. (b) RANGES AND *DEFAULT* VALUES OF ERROR MODEL PARAMETERS FOR MULTIPLICATIVE ERROR BIAS (mu), LOG-ERROR STANDARD DEVIATION (σ), AND LOG-ERROR TEMPORAL CORRELATION (ρ^2) FOR PM AND IR SENSOR RETRIEVALS. THE RANGE R_L OF THE UNIFORM DISTRIBUTION $U[0, R_L]$ FOR SAMPLING FALSE ALARMS WAS SET AT $R_L = 0.5$ mm/h FOR PM AND IR

	Probability of Rain Detection (P_1)		Probability of No-Rain Detection (P_0)
	Upper boundary (P_1=1.0)	Lower boundary (P_1=0.001)	
PM	5 mm/hr	0.2 mm/hr	0.98
IR	10 mm/hr	0.8 mm/hr	0.90

(a)

	Multiplicative Bias (mu)		Standard Deviation (log-error) (σ)		Correlation (log-error) (ρ^2)	
	Default	Range	Default	Range	Default	Range
PM	1.15	0.25–1.75	0.40	0.10–1.30	0.40	0.10–0.90
IR	1.15	-	0.70	0.5–0.90	0.40	-

(b)

for a Gaussian random variable leads to the following equations for the propagation of μ and σ^2:

$$\mu_i = \mu + (\rho)(\varepsilon_{i-1} - \mu)$$
$$\sigma_i^2 = \sigma^2(1 - (\rho^2)) \quad (5)$$

where time index i represents discrete hourly time step while ρ^2 is the lag-one autocorrelation of ε.

In the fourth outcome (false rain detection), the satellite (PM and IR) rain retrieval is statistically generated from a uniform distribution $U[0, R_L]$ representing an acceptable range of low intensity rainfall estimates usually occurring in false rain detection. The R_L parameter was assigned a low value of 0.5 mm/h for both PM and IR sensor retrievals, which are similar to the false alarm rain rates suggested by Guetter *et al.* [15].

As discussed earlier in this section, SREM is used to statistically simulate multiple realizations of satellite rainfall retrievals over Posina basin using observations from a dense rain gauge network as the basis for reference basin-averaged rainfall. The algorithm structure is shown in Fig. 4. The algorithm is applied at discrete hourly time steps (defined by time index i). The probabilities of rain detection (P_1) and no rain detection (P_0) are modeled through Bernoulli distributions $B(1, P_1)$ and $B(1, P_0)$, respectively, in a fashion similar to [15]. Table I summarizes the PM and IR retrieval error characteristics considered in this paper. The satellite rain and no-rain detection probabilities and the false alarm rain rate parameter values are shown in Table I(a). The satellite's multiplicative bias (mu), log-error standard deviation (σ) and autocorrelation parameter (ρ^2) were varied across a range of values shown in Table I(b). A set of "*default*" values was also assigned to facilitate relative comparisons between the varied error parameter values. These *default* values are deemed error parameters associated with realistic levels of satellite retrieval accuracies. On the basis of past studies, the default values of $mu(\sigma)(\rho^2)$ for PM and IR retrievals were assigned as 1.15(0.40)(0.40) and 1.15(0.70)(0.40), respectively. From (3) and (4), it can be shown that our selected default values are in fact equivalent to a standard error of 45% for PM and 90% for IR retrievals. Kummerow *et al.* [9] have shown that PM retrievals can be biased in the ranges of 15% to 20% overland, while Negri and Adler [24] have reported rms error for IR retrievals at the range of 100% to 200% at hourly time scale.

The primary distinction between PM and IR retrievals is represented in this error model through P_1, the satellite rain estimation error statistics (in particular the conditional error variance), and to a lesser effect by P_0. By assigning higher upper/lower rain thresholds for IR in (1), the probability of IR rain (false no-rain) detection becomes consistently lower (higher) than that of the PM retrieval. The lower P_0 will lead to rate of higher false alarms, which is typical in IR retrievals. Furthermore, the two times higher standard error adequately characterizes the higher degree of IR rain estimation uncertainty with respect to PM retrieval.

IV. SIMULATION FRAMEWORK

The hydrologic model parameters were calibrated based on the optimization algorithm of Duan *et al.* [25] for three time resolutions (hourly, 3-h, and 6-h time steps) using the rain gauge basin-averaged rainfall as input to TOPMODEL. The simulated hydrograph based on the hourly TOPMODEL parameters and *reference rainfall* input was considered to represent the most accurate rainfall-runoff transformation for the basin, and was used as reference for the subsequent error analysis (henceforth

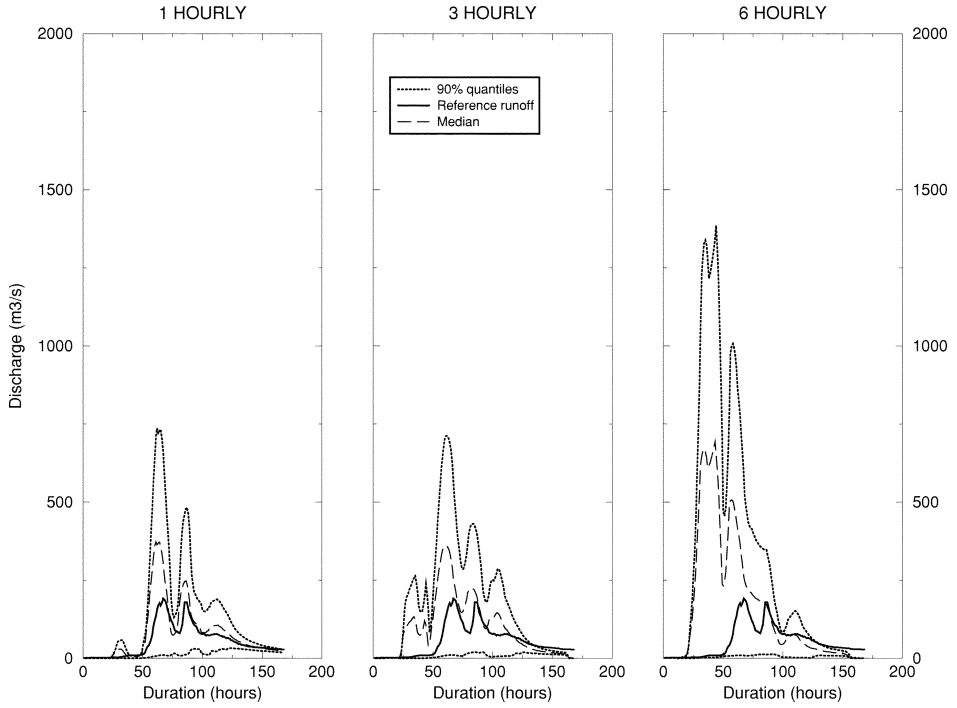

Fig. 5. Flood prediction uncertainty for hourly, 3-, and 6-h PM retrievals for the October 1992 storm event in Posina. The quantiles shown are the 50% (median), and the confidence bounds of 5% and 95% (90% area).

called the "*reference runoff*"). Because the correlation with observed runoff was very high (0.92), comparisons of *reference runoff* with runoff predictions driven by different synthetic satellite retrieval inputs would indicate the adequacies of the retrieval scheme and its impact on flood prediction uncertainty. The simulation exercise consisted of making multiple runs (i.e., realizations) of the hydrologic model, each with a random realization of synthetic satellite rain retrievals derived from SREM, and evaluating error statistics at the level of flood prediction. Three errors that adequately characterize uncertainty in flood prediction are evaluated: 1) mean absolute error in peak runoff; 2) mean absolute error in time to peak; and 3) mean absolute error in runoff volume. The error in these three flood hydrograph parameters is defined as

$$\begin{aligned}&\text{Error in Peak Runoff}\\&=\frac{1}{N_{\text{sim}}}\\&\cdot\sum_{i=1}^{N_{\text{sim}}}\left|\frac{\text{Peak Runoff}_i-\text{Peak Runoff}_{\text{ref}}}{\text{Peak Runoff}_{\text{ref}}}\right|\\&\text{Error in Time to Peak}\\&=\frac{1}{\text{N}_{\text{sim}}}\\&\cdot\sum_{\text{i}=1}^{\text{N}_{\text{sim}}}\left|\frac{\text{Time to Peak}_{\text{i}}-\text{Time to Peak}_{\text{ref}}}{\text{Time to Peak}_{\text{ref}}}\right|\\&\text{Error in Runoff Volume}\\&=\frac{1}{\text{N}_{\text{sim}}}\\&\cdot\sum_{\text{i}=1}^{\text{N}_{\text{sim}}}\left|\frac{\text{Runoff Volume}_{\text{i}}-\text{Runoff Volume}_{\text{ref}}}{\text{Runoff Volume}_{\text{ref}}}\right|\end{aligned}\tag{6}$$

where N_{sim} is the total number of simulation runs (satellite realization of retrievals); subscript i indicates the simulation index; and subscript ref signifies the hydrologic parameter was derived from the *reference runoff*.

A. Assessment of PM Retrievals

We used the above simulation framework to investigate how PM sampling and retrieval error characteristics interact in the runoff transformation process (characterized by the three runoff error parameters in (6). For each investigated scenario, 20 000 N_{sim} realizations were performed, and synthetic satellite retrievals propagated through the calibrated hydrologic model to derive ensemble runoff simulations. Our preliminary study with synthetic satellite retrievals indicated 20 000 model runs to be the minimum Monte Carlo sample size beyond which the error statistics in runoff showed insignificant variability. For both the 3- and 6-h scenarios, a second-degree polynomial interpolation was performed to interpolate the runoff at hourly scales. A point to note is that a satellite may not overpass a watershed exactly at the start of a storm event, but may initiate sampling with a delay. Thus, considering delays rounded off to the nearest hour, there may be a maximum of 2-h delay for the 3-h sampling, while for the 6-h sampling the delay can be up to 5 h. To account for this effect we repeated the simulation exercise for these possible sampling-initiation patterns (three patterns for the 3-h and six patterns for 6-h sampling scenarios). The errors in runoff parameters for the 3- and 6-h sampling scenarios were normalized by the corresponding runoff simulation error of the hourly sampling scenario to derive *error ratios* (ERs) for the different error parameters as follows:

$$\begin{aligned}E.R_{3-\text{hourly}}&=\frac{\text{Error in Runoff}_{3-\text{hourly}}}{\text{Error in Runoff}_{\text{hourly}}}\\E.R_{6-\text{hourly}}&=\frac{\text{Error in Runoff}_{6-\text{hourly}}}{\text{Error in Runoff}_{\text{hourly}}.}\end{aligned}\tag{7}$$

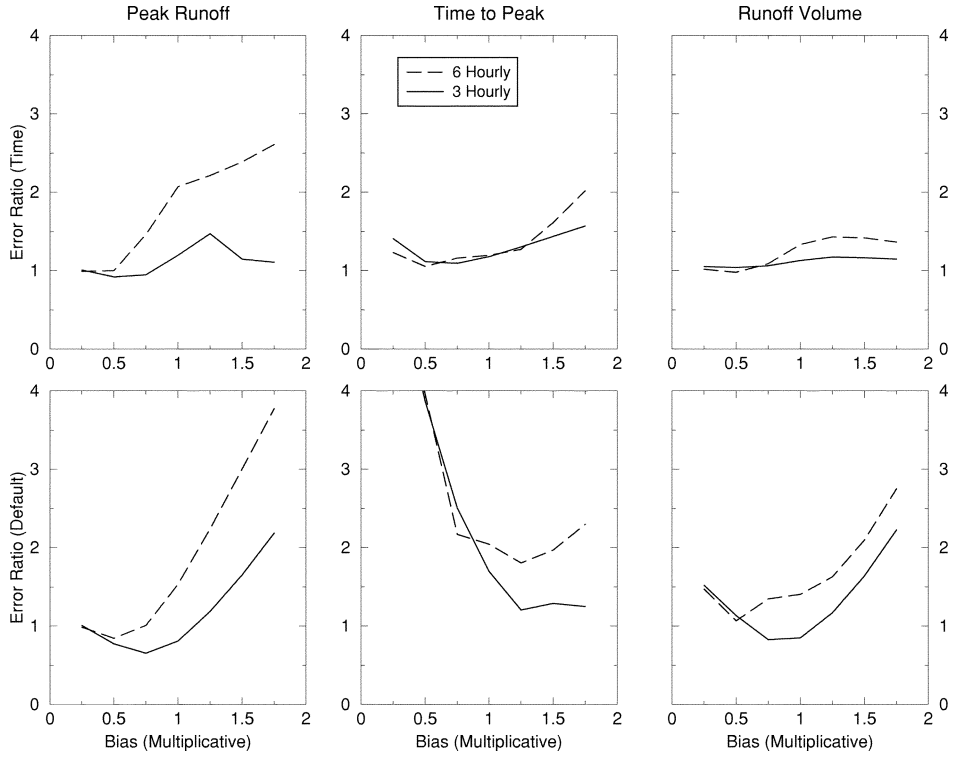

Fig. 6. Effect of PM retrieval bias (multiplicative) on flood prediction uncertainty presented in terms of ERs. (Top) *Time ERs:* ratio of runoff error for a given sampling scenario (3 or 6 h) normalized by the 1-h runoff error derived from the correspondingly varied retrieval error parameters. (Bottom) *Default ER:* ratio of runoff error for a given sampling scenario (3 or 6 h) normalized by the 1-h runoff error with the default retrieval error parameters. The upper panels show the effect of sampling, and the lower panels show the combined effect of sampling and retrieval error on flood prediction uncertainty.

The ERs shown above allow comparison of 3- and 6-h sampling to a common reference of hourly sampling, which is typically used in hydrologic forecasting of floods. ER sensitivity to satellite retrieval error parameters (mu, σ, and ρ^2) for the 3- and 6-h sampling scenarios is evaluated to study the effect of sampling and retrieval error interaction in the runoff transformation process. Two measures are used, both of which represent the ratio of runoff simulation errors for the 3- and 6-h sampling scenarios to those from the hourly sampling scenarios. The *Default ER* statistics use the varying values of the error measures in Table I(b) for the 3- and 6-h scenarios, but the default values for the hourly scenario. This allows the evaluation of the combined effect of retrieval and sampling error on flood prediction uncertainty. In order to isolate the effect of the sampling error, the *Time ER* statistics use the same (varying) values of the error measures from Table I(b) for both 3- or 6-h and hourly scenarios.

The impact of PM sampling frequency on flood prediction uncertainty is presented in Fig. 5, which shows the "*reference*" hydrograph of the catastrophic flood event with the 5%, 50%, and 95% quantiles of the satellite predicted hydrographs derived from the simulation exercise run with the default PM retrieval error parameters shown in Table I(a) and (b). Compared to the 6-h scenario, the 3-h has significantly (about half) lower flood prediction uncertainty, which appears to be comparable to the hourly sampling scenario. The 6-h sampling scenario would overestimate peak runoff by up to 1500 m^3/s, a magnification of about eight times the observed value, and underestimate the time to peak by 15 h. This tremendous overestimation of the flood wave by 6-h sampling further underscores the importance of more frequent sampling for storms of such magnitude.

In the subsequent three figures [6]–[8], we demonstrate the sensitivity of flood prediction uncertainty (*Default ER*: lower panels; *Time ER*: upper panels) to PM retrieval error characterized by varying values of multiplicative bias (mu), standard deviation of log-error (σ), and lag-one correlation (ρ^2), respectively. In varying one of the error parameters in this sensitivity experiment, the other PM error parameters are set to their default value shown in Table I(b).

Several features are worth noting from these figures, starting with Fig. 6. It is observed that ER generally reaches a minimum at moderate retrieval bias conditions. The observation that the minimum ER does not occur at no bias ($mu = 1.0$), but at moderate bias condition, is expectable, as random error in rainfall retrieval may introduce biases in runoff simulation [14]. The 3-h sampling exhibits minimum ERs at bias values closer to 1 than the 6-h counterpart, indicating that sampling can magnify the effect of retrieval error in runoff. We observe that the *Time ER* in runoff volume is nearly insensitive to the retrieval bias, which is expected as *Time ER* represents the effect of sampling alone and runoff volume is a time-integrated hydrologic parameter with a tendency to compensate for random input errors in time. This indicates that water balance studies for a medium-sized watershed can be well represented by 3- and 6-h PM observations provided the retrieval scheme performs at the levels assumed here. Sampling error, though, can significantly affect peak runoff error (and to a lesser effect time-to-peak error) as *Time ER* is shown to reach 2.5 (2.0) for the peak runoff (time-to-peak) in the 6-h sampling scenario, while for the 3-h scenario the effect is moderate to negligible. Another observation is that the rate of increase of ER (both *Time* and *Default*) with increasing bias is

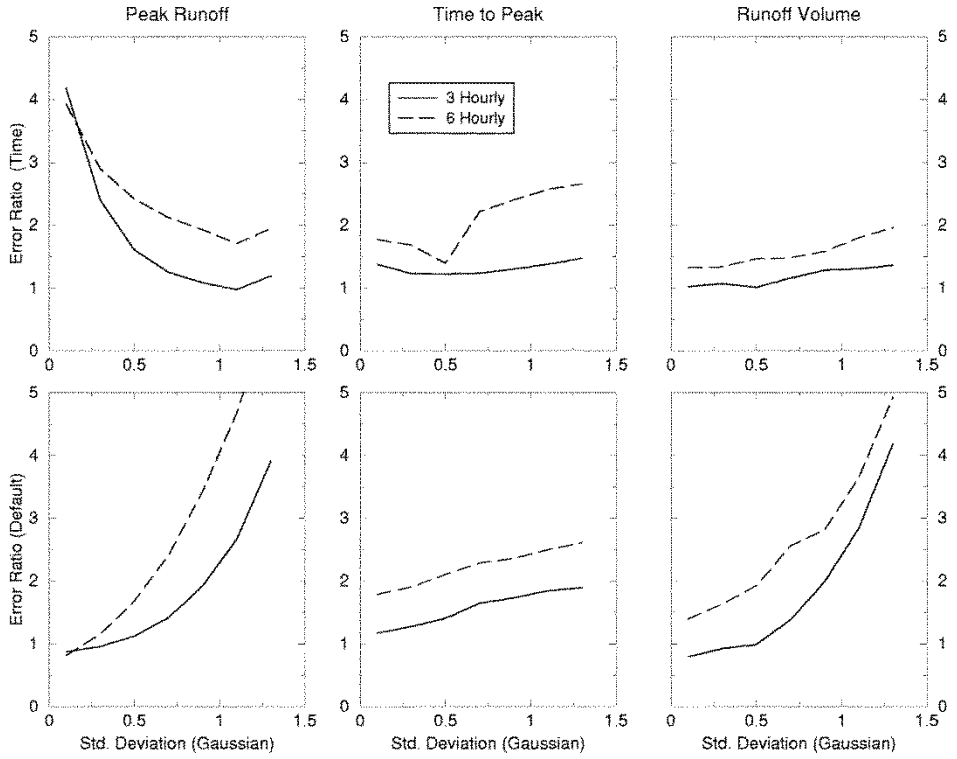

Fig. 7. Effect of PM retrieval error standard deviation (σ) on flood prediction uncertainty presented in terms of ERs. (Top) *Time ERs:* ratio of runoff error for a given sampling scenario (3 or 6 h) normalized by the 1-h runoff error derived from the correspondingly varied retrieval error parameters. (Bottom) *Default ER:* ratio of runoff error for a given sampling scenario (3 or 6 h) normalized by the 1-h runoff error with the default retrieval error parameters. The upper panels show the effect of sampling, and the lower panels show the combined effect of sampling and retrieval error on flood prediction uncertainty.

stronger in overestimation ($mu > 1$), and again more so for the 6-h sampling scenario, as indicated by the steeper gradients and the widening difference between 3- and 6-h ER plots. This indicates that there exists a higher degree of error interaction with sampling when the sensor overestimates rainfall, which is consistent with past findings [26].

In Fig. 7 (upper panels), *Time ER* indicates that increasing the retrieval error standard deviation obscures the error due to sampling on peak runoff prediction. However, this effect is not apparent at the time-to-peak and runoff volume *Time ER* plots, which seem to only slightly increase relative to the retrieval random error. As with Fig. 6, the 6-h sampling is associated with higher values of *Time ER* values than those of the 3-h, which range from 1 to 1.5 for the time-to-peak and runoff volume parameters. In the *Default ER* plots (lower panels of Fig. 7), which show the combined effect of sampling and retrieval error, we observe that the 6-h sampling is consistently higher than 3-h sampling error by a factor of 1.2 or higher. The *Default ER* plot for peak runoff exhibits a steeper rate of increase in the 6-h sampling scenario relative to the corresponding 3-h scenario.

In Fig. 8 we show that the *Default ER*s (lower panels) for all three runoff parameters are nearly insensitive to the temporal correlation of the retrieval error (ρ^2) for both 3- and 6-h sampling scenarios. This indicates that the time lag (minimum of 3 h) between PM observations is long enough to minimize potential effects from temporally correlated errors. At the hourly time scale, though, the rain retrieval error correlation can play a role in runoff prediction error. This is because correlation would indirectly increase the systematic error in the retrieval, which would consequently lead to an increase in runoff error parameters. This effect is apparent in the *Time ER* plots of the upper panels of Fig. 8, which are shown to decrease (peak runoff has the steepest descent) with increasing the temporal correlation of the retrieval error.

Fig. 9 presents contour plots of the *Time ER* values for covariations of the retrieval error temporal correlation and standard deviation for 3- and 6-h sampling scenarios (left and right panels of Fig. 9, respectively). The patterns of ER values are the same in both contour plots, but the magnitudes of the *Time ER* values associated with the 6-h sampling are almost double those of the 3-h sampling. The nearly circular nature of contours indicates that the temporal correlation and standard deviation contribute roughly equally to the magnitude of the *Time ER*. A maximum point ($Time\ ER > 2.00$ for 3-h and > 5.00 for 6 h) is observed at standard deviation (σ) of 0.3 and lag one correlation (ρ^2) of 0.1. At high retrieval errors ($\sigma > 0.6$, and $\rho^2 > 0.6$), we observe the error ratios reaching lower values (1.1 in 3-h and 2.0 in 6-h). These lower values are caused by relatively higher increase in errors derived from the hourly sampling. This indicates that the error due to sampling alone tends to become obscured by the higher error in rainfall retrieval for both 3- and 6-h sampling scenarios. Consequently, at such high levels of retrieval error, it would not matter what the sampling frequency is—the algorithm performs too poorly to have any benefit in runoff simulation accuracy by increased sampling. It is therefore important to ensure that the PM retrieval algorithms perform at adequate levels of retrieval accuracy to maximize the benefit achieved in flood prediction by any increase in sampling frequency.

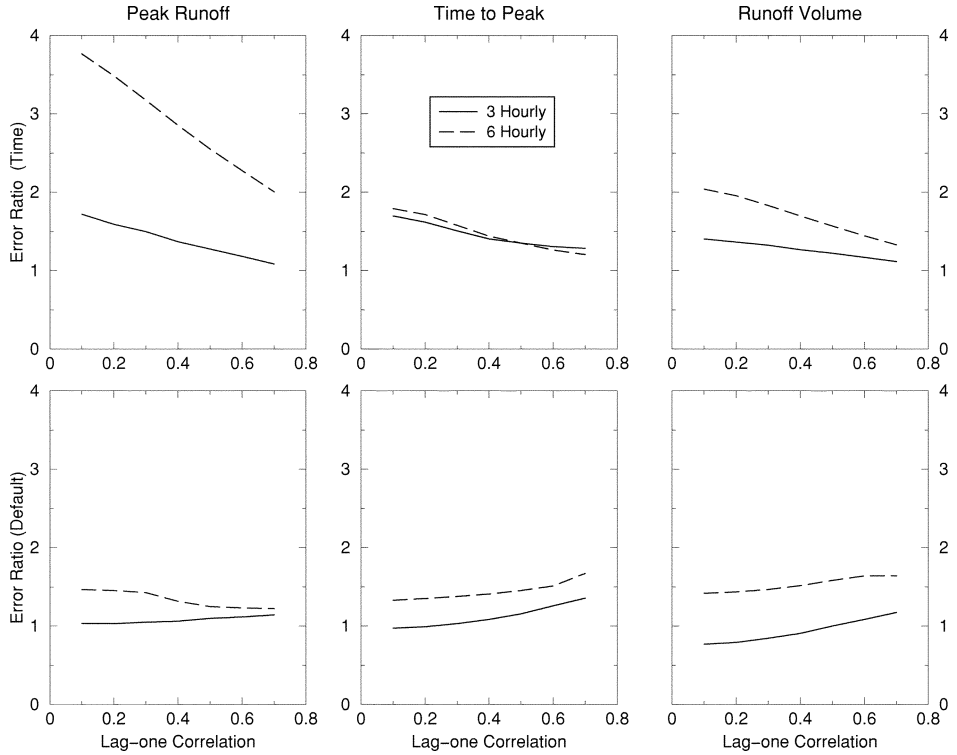

Fig. 8. Effect of PM retrieval error lag-one correlation (ρ^2) on flood prediction uncertainty presented in terms of ERs. (Top) *Time ERs:* ratio of runoff error for a given sampling scenario (3 or 6 h) normalized by the 1-h runoff error derived from the correspondingly varied retrieval error parameters. (Bottom) *Default ER:* ratio of runoff error for a given sampling scenario (3 or 6 h) normalized by the 1-h runoff error with the default retrieval error parameters. The upper panels show the effect of sampling, and the lower panels show the combined effect of sampling and retrieval error on flood prediction uncertainty.

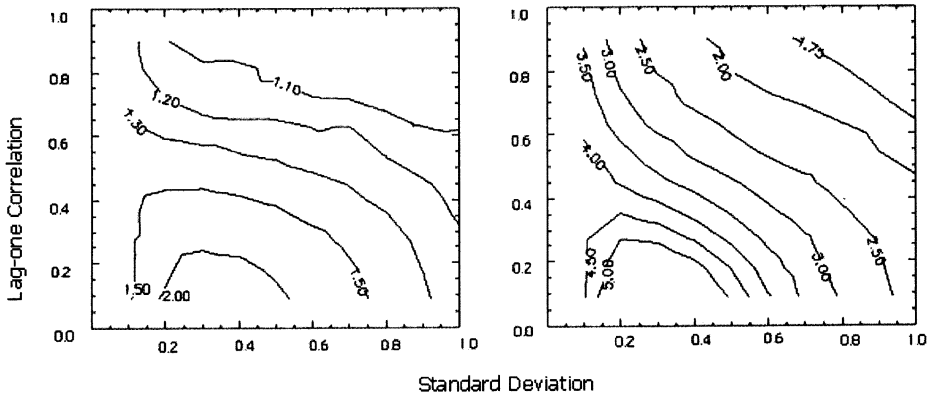

Fig. 9. Contours of peak runoff *Time ERs* in peak runoff as function of PM retrieval log-error's lag-one correlation (ρ^2) and standard deviation (σ) for 3-h (left panel) and 6-h (right panel) sampling scenarios.

B. Assessment of Combined PM-IR Retrievals

We also used the simulation framework to assess the impact of combining IR and PM retrievals in flood prediction. Considering three different levels of IR retrieval error (σ_{IR}: 0.5, 0.7 and 0.9), the utility of IR merging with PM was studied for varying levels of PM retrieval error (σ_{PM}: 0.1, 0.2, 0.3, 0.4, and 0.5). In all cases, the retrieval biases and lag-one correlation for both IR and PM were fixed at their *Default* value Table I(b). The IR rainfall was used as input to the hydrologic model at hours with no PM measurement, while the simulation framework was as mentioned above. A statistical assessment of the merged IR and MW rainfall input relative to the MW-only scenario is defined based on the following error ratios (named *Merging ER*) for the 3- and 6-h sampling

$$\text{Merging E.R}_{3\text{hourly}} = \frac{\text{Error in runoff}_{\text{mergedIR}-\text{PM}}}{\text{Error in runoff}_{3-\text{hourlyPM}}}$$
$$\text{Merging E.R}_{6\text{hourly}} = \frac{\text{Error in runoff}_{\text{merged IR}-\text{PM}}}{\text{Error in runoff}_{6-\text{hourlyPM}}} \quad (8)$$

The error in runoff indicates the error statistics of each of the three runoff-parameters, as defined in (6). A *Merging ER* value of less than one would indicate that the use of IR rainfall during hours with no PM observations reduces uncertainty in flood prediction.

Fig. 10 shows the effect of combining IR with PM retrievals on reduction of flood prediction uncertainty. *Merging ER* [(8)]

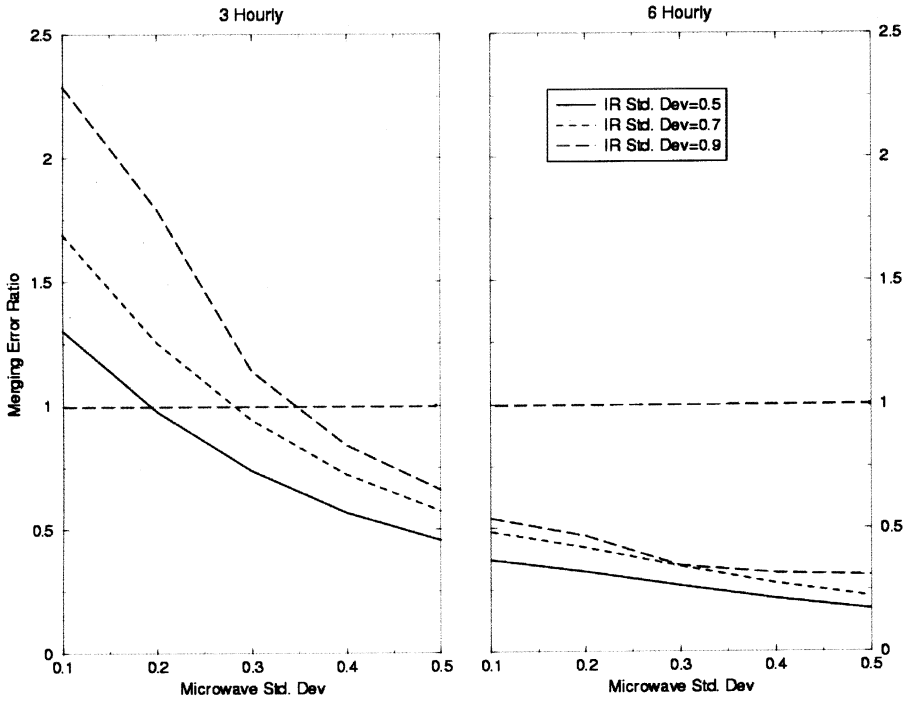

Fig. 10. *Merging ER* values of runoff volume presented as function of PM retrieval error standard deviation ($\sigma_{\rm PM}$) for two PM sampling scenarios (left panel: 3 h; right panel: 6 h) and three levels of IR retrieval error standard deviations ($\sigma_{\rm IR}$).

values shown for runoff volume are presented as function of PM retrieval error standard deviation for three levels of IR retrieval error standard deviations as discussed earlier. The rest of the parameters of the IR and PM retrieval error model are set to the default values in Table I(a) and (b). We observe that at low PM retrieval errors (standard deviation ($\sigma_{\rm PM}$): 0.20–0.35) the use of the more erroneous IR retrieval (standard deviation ($\sigma_{\rm IR}$): 0.5, 0.7, and 0.9) can actually increase flood prediction uncertainty for the 3-h sampling scenario (*Merging ERs* ranging from 1.25–2.25). This indicates that when the difference between IR-PM retrieval error standard deviations is within the range of 0.30–0.55, merging with IR retrievals would generally fail to achieve any beneficial effect on flood prediction accuracy for a 3-h PM sampling. As the difference between PM and IR retrieval error variances narrows, the use of IR retrievals become effective in reduction of flood uncertainty for the 3-h case. In contrast, we observe that the use of IR rainfall jointly with 6-h PM rainfall retrievals (right panel, Fig. 10) invariably reduces flood prediction uncertainty at all ranges of IR and PM retrieval errors considered in this paper. This is explained from the fact that the error due to infrequent sampling is so high in the 6-h case (as shown in Fig. 4) that any additional rainfall information from an IR sensor at the hourly scale becomes always beneficial in constraining that uncertainty in flood prediction. The relative reduction in uncertainty for the 6-h sampling scenario ranges from 50% to 80% (*Merging ERs*: 0.5–0.2, respectively), while for the 3-h scenario the reduction of uncertainty can be up to 50% (*Merging ERs*: 0.5) for high PM retrieval error. This reduction for 3-h PM sampling with the use of hourly IR retrievals draws the uncertainty level closer to that achieved by hourly PM sampling when compared with that derived from 3-h PM sampling alone.

V. Summary and Conclusion

This paper studied the sensitivity of satellite retrieval and sampling error on flood prediction uncertainty for a week-lasting rainfall event over a medium-sized watershed of a typical sensor footprint size ($\sim$ 100 km^2). We showed that a 3-h PM sampling is comparable to the hourly sampling in terms of flood prediction uncertainty for the major storm event, while uncertainty was shown to increase by a factor of 2–3 times for a 6-h sampling. Runoff uncertainty was found sensitive to both, systematic and random error components of PM retrievals. Particularly, the 6-h scenario was found to exhibit much higher sensitivity, especially when rainfall is overestimated. The effects of temporal correlation of retrieval error effects alone were not found to be significant for either 3- or 6-h sampling, but their strong interaction with error variance was evident. For estimation of runoff volume or water balance studies at the medium-sized watershed scale from overpassing PM sensors, the loss in accuracy due to sampling was found to be minimal. However, this was not the case for estimation of other flood hydrograph parameters like time-to-peak and peak runoff. At high errors of PM rainfall retrievals, the runoff error due effects of sampling alone was shown to become obscured by the retrieval error. Application of IR retrieved rainfall jointly with PM retrievals was shown to reduce flood prediction uncertainty consistently for the 6-h PM sampling scenario. In the 3-h sampling scenario, the potential runoff error reduction was shown to depend on the relative accuracy of IR retrieval with respect to the PM. The reduction in flood prediction uncertainty was found to range from 50% to 80% and up to 50% for 6- and 3-h sampling scenarios, respectively.

This study was limited to PM sampling scenarios of fixed revisit times (3 and 6 h) between successive overpasses. While

this is an expected sampling scenario for the GPM in the time frame of 2008 onward, current constellation of PM sensors (comprising a smaller array of satellites) sample rainfall events with variable revisit times ranging from 1–10 h [3]. As ungauged watersheds affected by flood problems are spread wide within the tropics, it would be necessary to calibrate the retrieval error parameters based on observed PM and IR sensor data matched at a more global scale. Our current study has been conditioned on sensor rain retrieval assumptions based on previous studies/results. Calibration with real sensor data is important to verify several of the key assumptions made during the formulation of SREM including: 1) the probability distribution of PM rainfall retrievals during false alarms; 2) the functional form of rain detection probability; and 3) the magnitudes of retrieval bias, error variances, and temporal correlation. There is also need to understand the effect of storm morphology (storm duration, fractional rain coverage, and rain rate variability) on satellite-based flood prediction uncertainty. Certainly, this information would be useful in identifying the potential subset of storm systems not suitable for flood prediction by satellite data. Future research should therefore address those issues to make a better assessment of satellite rainfall remote sensing for flood prediction of ungauged watersheds.

REFERENCES

[1] E. A. Simpson, C. Kummerow, W. K. Tao, and R. F. Adler, "On the Tropical Rainfall Measuring Mssion (TRMM)," *Meteorol. Atmos. Phys.*, vol. 60, pp. 19–36, 1996.

[2] NASA, "AQUA brochure," Goddard Space Flight Center, Greenbelt, MD, NP 2002-1-422.

[3] E. A. Smith, "Satellites, orbits and coverages," in *Proc. IGARSS*, Sydney, Australia, July 9–13, 2001.

[4] M. Flaming, "Requirements of the global precipitation mission," in *Proc. IGARSS*, Toronto, ON, Canada, June 24–28, 2002.

[5] S. Bidwell, J. Turk, M. Flaming, C. Mendelsohn, D. Everett, J. Adams, and E. A. Smith, "Calibration plans for the global precipitation measurement," in *Proc. Joint 2nd Int. Microwave Radiometer Calibration Workshop and CEOS Working Group on Calibration and Validation*, Barcelona, Spain, Oct. 9–11, 2002.

[6] S. Yuter, M.-J. Kim, R. Wood, and S. Bidwell. (2003, Feb.) Error and uncertainty in precipitation measurements. *GPM Monitor* [Online] Available: http://gpm.gsfc.nasa.gov/Newsletter/february03/calibration.htm.

[7] M. Grecu and E. N. Anagnostou, "Overland precipitation from TRMM passive microwave observations," *J. Appl. Meteorol.*, vol. 40, no. 8, pp. 1367–1380, 2001.

[8] A. Y. Hou, S. Zhang, A. da. Silva, W. Olson, C. Kummerow, and J. Simpson, "Improving global analysis and short range forecasts using rainfall and moisture observations derived from TRMM and SSM/I passive microwave sensors," *Bull. Amer. Meteorol.*, vol. 82, 2001.

[9] C. Kummerrow, Y. Hong, W. S. Olson, S. Yang, R. F. Adler, J. McCollum, R. Ferraro, G. Petty, D.-B. Shin, and T. T. Wilheit, "The evolution of the goddard profiling algorithm (GPROF) for rainfall estimation from passive microwave sensors," *J. Appl. Meteorol.*, vol. 40, pp. 1801–1820, 2001.

[10] Q. Xiao, X. Zou, and Y. H. Kuo, "Incorporating the SSM/I derived precipitable water and rainfall rate into numerical model: A case study for ERICA IOP-4 cyclone," *Mon. Weather Rev.*, vol. 128, pp. 87–108, 2000.

[11] G. W. Petty and W. F. Krajewski, "Satellite estimation of precipitation over land," *Hydrol. Sci. J.*, vol. 41, pp. 433–451, 1996.

[12] M. Winchell, H. V. Gupta, and S. Sorooshian, "On the simulation of infiltration- and saturation excess runoff using radar-based rainfall estimates: Effects of algorithm uncertainty and pixel aggregation," *Water Resources Res.*, vol. 34, no. 10, pp. 2655–2670, 1998.

[13] M. Borga, E. N. Anagnostou, and E. Frank, "On the use of real-time radar rainfall estimates for flood prediction in mountainous basins," *J. Geophys. Res.*, vol. 105, no. D2, pp. 2269–2280, 2000.

[14] F. Hossain, E. N. Anagnostou, T. Dinku, and M. Borga, "Hydrologic model sensitivity to parameter and radar rainfall estimation uncertainty," *Hydrol. Proc.*, 2004, to be published.

[15] A. K. Guetter, K. P. Georgakakos, and A. A. Tsonis, "Hydrologic applications of satellite data: 2. Flow simulation and soil water estimates," *J. Geophys. Res.*, vol. 101, no. D21, pp. 26 527–26 538, 1996.

[16] T. Dinku, E. N. Anagnostou, and M. Borga, "Improving radar-based estimation of rainfall over complex terrain," *J. Appl. Meteorol.*, vol. 41, pp. 1163–1178, Dec. 2002.

[17] B. Bacchi, R. Ranzi, and M. Borga, "Statistical characterization of spatial patterns of rainfall cells in extratropical cyclones," *J. Geophys. Res.*, vol. 101, no. D21, pp. 26 277–26 286, 1996.

[18] K. J. Beven and M. J. Kirkby, "A physically-based variable contributing area model of basin hydrology," *Hydrol. Sci. J.*, vol. 24, no. 1, pp. 43–69, 1979.

[19] K. J. Beven, R. Lamb, P. Quinn, R. Romanowicz, and J. Freer, "TOPMODEL," in *Computer Models of Watershed Hydrology*, V. P. Singh, Ed. Fort Collins, CO: Water Resource, 1995, pp. 627–668.

[20] G. J. Huffman, R. F. Adler, E. F. Stocker, D. T. Bolvin, and E. J. Nelkin, "Analysis of TRMM 3-hourly multi-satellite precipitation estimates computed in both real and post-real time," in *Proc. 12th Conf. Satellites, Meteorology and Oceanograpy*, Long Beach, CA, Feb. 9–13, 2003.

[21] A. J. Negri, R. F. Adler, and L. Xu, "A TRMM-calibrated infra-red rainfall algorithm applied over Brazil," *J Geophys. Res.*, vol. 107, no. D20, 2002.

[22] M. Grecu, E. N. Anagnostou, and R. F. Adler, "Assessment of the use of lightning information in satellite infra-red rainfall estimation," *J. Hydrometeorol.*, vol. 1, pp. 211–221, 2000.

[23] A. A. Tsonis, G. N. Triantafyllou, and K. P. Georgakakos, "Hydrological applications of satellite data 1. Rainfall estimation," *J. Geophys. Res.*, vol. 101, no. D21, pp. 26 517–26 525, 1996.

[24] A. J. Negri and R. F. Adler, "An inter-comparison of three satellite rainfall techniques over Japan and surrounding waters," *J. Appl. Meteorol.*, vol. 32, pp. 357–373, 1993.

[25] Q. S. Duan, S. Sorooshian, and V. K. Gupta, "Effective and efficient global optimization for conceptual rainfall-runoff models," *Water Resources Res.*, vol. 28, pp. 1015–1031, 1997.

[26] E. N. Anagnostou and F. Hossain, "Assessment of the impact of satellite sampling and rainfall estimation uncertainty on runoff simulation for a mountainous watershed," presented at the *Proc. EGS (European Geophysical Society) Pilinius Symp.*, Siena, Italy, 2001.

Faisal Hossain received the B.S. degree in civil engineering from the Institute of Technology, Banaras Hindu University, Varanasi, India, and the M.Eng. degree from the National University of Singapore in water and waste water engineering, in 1996 and 1999, respectively. He is currently pursuing the Ph.D. degree at the University of Connecticut, Storrs, in environmental engineering.

His field or research is on remote sensing of rainfall-based flood prediction uncertainty.

Emmanouil N. Anagnostou received the B.S. degree in civil engineering from the National Technical University, Athens, Greece, and the M.S. and Ph.D. degrees from The University of Iowa, Ames, both in hydrometeorology.

He is currently an Associate Professor in the Department of Civil and Environmental Engineering, University of Connecticut, Storrs. His current research interests include hydrologic remote sensing and its applications in hydrology and water resources.

Tufa Dinku received the B.S. degree from the University of Addis Ababa, Addis Ababa, Ethiopia, and the M.S. degree in civil engineering from the University of Connecticut, Storrs. He is currently pursuing the Ph.D. degree at the University of Connecticut, Storrs.

His field of research is on multisensor rainfall estimation.